

Observation of defects on insulator surfaces following bombardment with slow Kr^{35+} , Xe^{44+} , Th^{74+} , and U^{70+} ions

D. Schneider *, M.A. Briere, J. McDonald and W. Siekhaus

Lawrence Livermore National Laboratory, P.O. Box 808, L-421, Livermore, CA 94550, USA

We found unambiguous evidence of a new radiation effect from the occurrence of single ion defects which are created through the interaction of the Coulombic potential of slow highly charged ions (e.g. Xe^{44+} and U^{70+}) and the surface of solid insulating materials (i.e. mica). In the cases studied, the kinetic energy of the ions is some 300–500 keV (ca. 2.2 keV/u), while the energy associated with the electrostatic potential of the incident ions approaches 200 keV. Defect production in mica has been investigated as a function of incident ion charge using an atomic force microscope. The volume of “blister-like” defects has been found to be proportional to the incident ion charge.

1. Introduction

Presently, much effort is devoted towards the understanding of the interaction of slow very highly charged ions (SVHCI) with solid surfaces. The interest originates from several basic, as well as applied, physical issues. These include multi-electron capture and cascade processes occurring during ion neutralization, as well as possible nanometer scale lithographic applications due to ion induced surface modifications. These studies also provide information required for the understanding of ion–wall interactions, as encountered in fusion research and plasma processing. Beams of highly charged ions, up to U^{82+} , are now available from sophisticated ion sources such as EBIS(T) (electron beam ion source (trap)). The EBIT used here is described in detail in refs. [1–3]. Slow (several keV/u) very highly charged, high Z ions (SVHCI), e.g. U^{82+} , can carry up to several hundred keV potential energy. It is of fundamental interest how such ions lose their energy and neutralize, as they slowly approach the surface, as well as what kinds of defects they can cause in the solid target. In order to understand and study the physical properties and, in particular, the neutralization dynamics, secondary reaction products such as electrons [4], X-rays [5] and sputter ions [6,7] are measured and sophisticated model calculations are performed [8,9]. Here, first results from a study using an atomic force microscope (AFM) to investigate the types of defects that these SVHCI cause within the near

surface region of selected insulating solids are reported.

2. Experimental

In this paper, observations of surface defects on insulators, caused by highly charged slow ion impact, are reported (see ref. [10]), where the ions are produced with EBIT. The operation of an EBIT is only briefly addressed; its modification into a source by means of an efficient extraction system is described in detail in ref. [2]. EBIT is an electron beam ion trap, where the trap itself consists of a three segment axial drift tube assembly. These segments can be individually biased, high on the ends and low in the middle, to create an electrostatic well along the central axis. An electron beam, compressed to ~ 70 mm diameter in a 3 T magnetic field, travels along the central axis. The energy of the electrons is determined by an overall bias voltage applied to the drift tube assembly by a fast switching high voltage power supply (e.g. 5–20 kV). Electron beam currents are typically around 100 mA. Neutral gas molecules, such as Xe, are ionized by the beam within the central well of the drift tubes and are trapped radially by the space charge of the electron beam. These ions undergo successive ionization and other electron–ion and atom–ion interactions, which determine the achievable charge states in the trap. After a desired charge state equilibrium is reached, the ions are ejected from the trap via fast switching of the drift tube potentials (\sim ms), e.g. by ramping the central drift tube such that the potential well is diminished for a short time. The ejected ions are then momentum

* Corresponding author. Fax: 510-422-5940; telephone: 510-423-5940.

analyzed and focused onto a target surface. Collimation of the ion beam is achieved by a four-jaw slit arrangement and the beam spot size used is about 5 mm in diameter. The targets were mounted on a ladder with one position left open, containing a 5 mm diameter aperture, which was used to verify the beam flux and position as well as to optimize the incident beam current, by guiding the ions through it onto an open faced photomultiplier or microchannel plate array for detection. The ion detection efficiency varies between 30 and 60% depending upon the details of the detector system. The vacuum along the beam path and in the target area is about 5×10^{-9} Torr. The number of Xe^{44+} ions which were extracted, for example, in about 40 ms wide pulses was 10^5 ions/s with an exposed area of 0.2 cm^2 . Exposure of the targets for 1 h therefore resulted in a total fluence of about 10^9 ions/ cm^2 . The targets used were mica, LEXAN ($\text{C}_{16}\text{H}_{14}\text{O}_3$), and silica glass, which were cleaned with alcohol (LEXAN and glass) or, in the case of mica, one layer was cleaved off prior to mounting. After exposure, the targets were placed in a desiccator and kept under vacuum until they were mounted onto the target holder of the atomic force microscope (AFM). It should be noted that exposure to air of previously irradiated samples for periods of up to one year does not significantly influence the results of the AFM measurements on the nanometer scale, though increased dust particle contamination increases the occurrence of “tip crashes”. A Digital Instruments Nanoscope III AFM was used in the contact mode with SiN cantilevers having characteristic rigidities of between 0.1 and 10 nN/nm. The results presented here were produced using a cantilever with a nominal rigidity of about 1 nN/nm. Qualitatively, the results have been found not to depend on the rigidity or initial force settings of the microscope and essentially the same results are found using the non-contact reverberating tip AFM mode. The exposed areas were scanned over several regions of ca. 100 nm to 1 μm on a side with scans of unexposed areas performed for comparison.

3. Results and discussion

Microscopic studies have been performed to study the surface defects created by slow highly charged ion ($7 \text{ kV} \times q\text{Xe}^{44+}$, U^{70+}) impact on an insulator surface. The principle target used was mica ($\text{KAl}_3\text{Si}_3\text{O}_{10}(\text{OH})_2$), with a total incident ion dose of a few 10^9 ions/ cm^2 . The surface topology of the samples was then measured using an atomic force microscope (AFM). The results are shown in Figs. 1–3. From the areal density of observed “blisters” and the total number of ions, one can conclude that the “blisters” are produced by single ion impact.

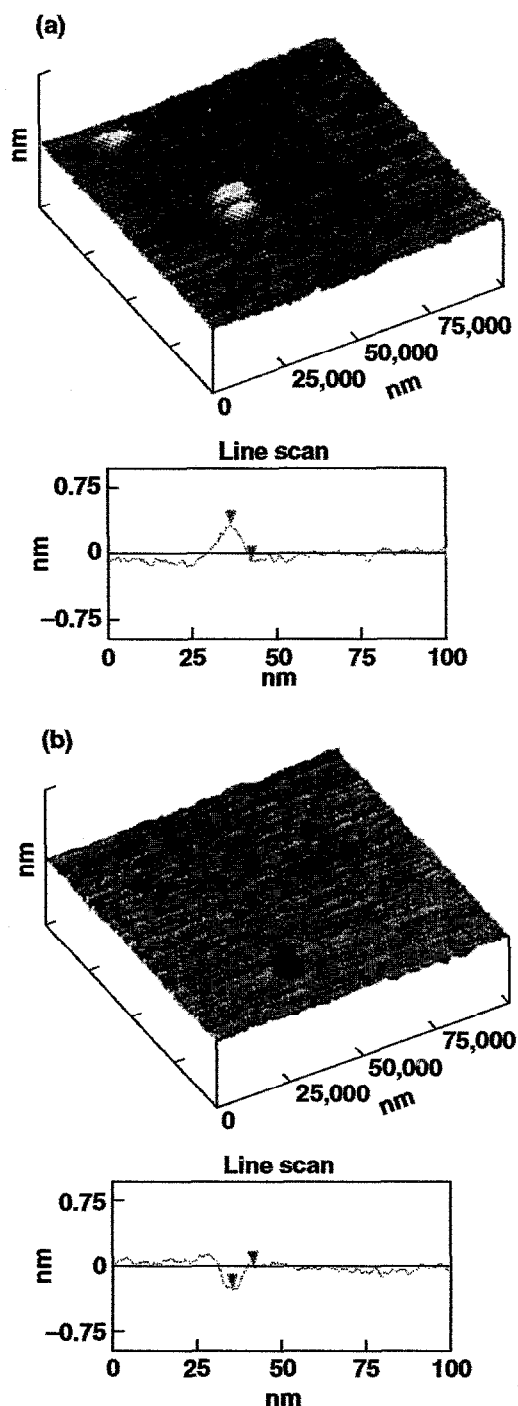


Fig. 1. Results from atomic force microscope scans following the bombardment of mica with slow (308 keV) Xe^{44+} ions, depicted in both perspective and line representations of (a) the results for an exposed area (dose 10^9 ions/ cm^2) after one scan, showing the presence of a “blister-like” defect; (b) a “blister” with its top “peeled” off by AFM tip of the same defect shown in (a).

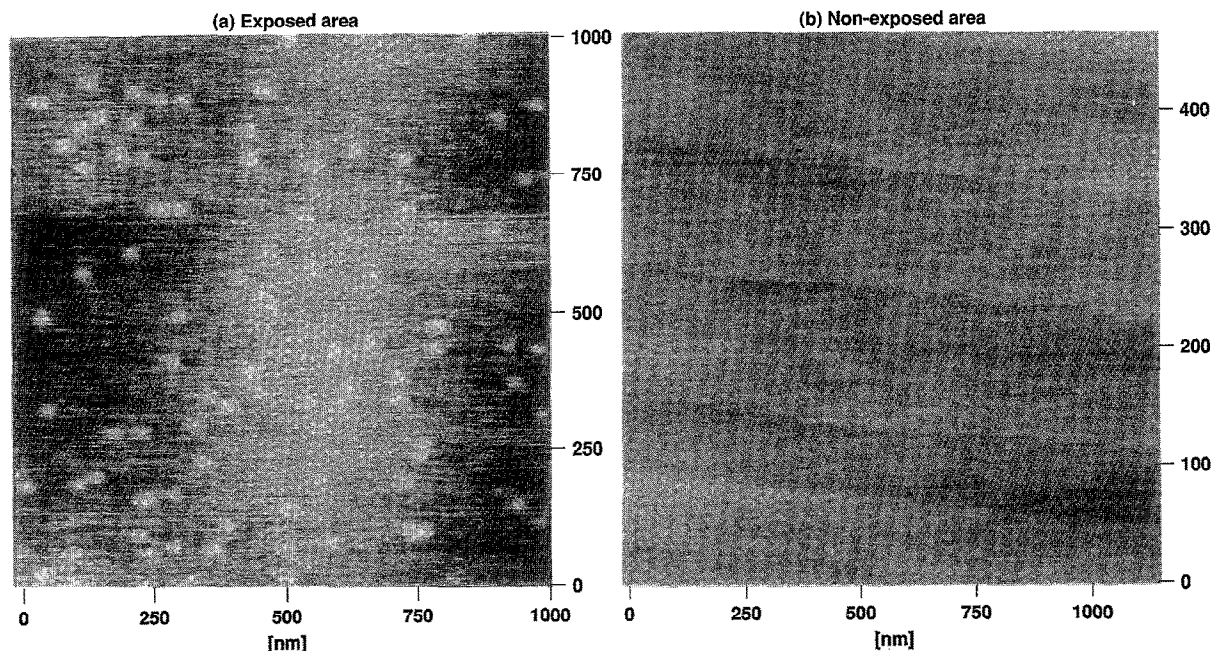


Fig. 2. Results of an atomic force microscope scan (a) following the bombardment of mica with slow (490 keV) U^{70+} ions (dose 10^9 ions/cm²); (b) non-exposed area.

Mica has a complex structure of negatively charged alumino-silicate layers, involving both tetrahedra and octahedra, with intermediate layers of positive ions, usually potassium, providing charge neutrality to the mineral. The electrostatic forces between the positive ions and negatively charged layers make mica a “hard” mineral with characteristic cleavage behavior.

Perspective view topological reconstructions, as well as profile line scans, from AFM measurements over exposed areas using Xe^{44+} are shown in Figs. 1a and b. The height of the observed “blisters” is about 0.4 nm

(Fig. 1a) with a base diameter of about 10 nm. It is interesting to note that, through multiple scans of the tip of the AFM over the same area, it is possible to flatten or completely remove the top layer of the “blister”, revealing a “pit” underneath (Fig. 1b). It has been found that this peeling process is sample dependent and that most samples do not display this behavior, regardless of the cantilever rigidity or initial applied force of the microscope. It has also been determined that the formation of the “pits” is not an artifact of the direction of the AFM measurement

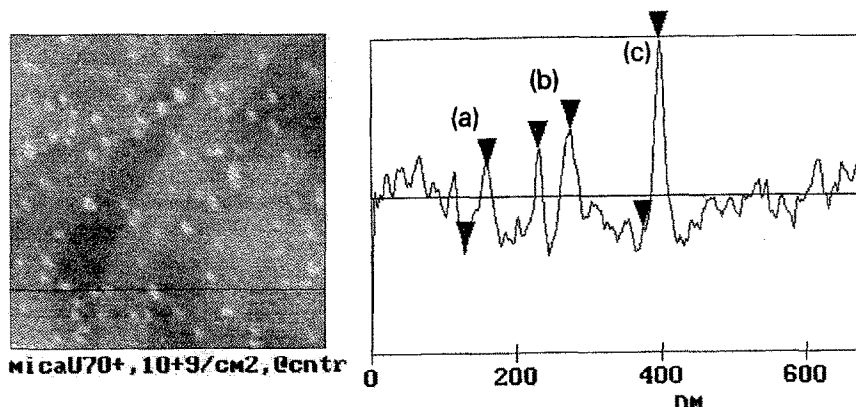


Fig. 3. Results of an atomic force scan following the bombardment of mica with slow (490 keV) U^{70+} ions (dose 10^9 ions/cm²). (a) Horizontal distance 30.815 nm; vertical distance 0.2602 nm; angle 0.4838°. (b) Horiz. distance 44.510 nm; vert. distance 0.0632 nm; angle 0.0813°. (c) Horiz. distance 22.255 nm; vert. distance 0.5942 nm; angle 1.5295°. FFT period dc; FFT amplitude 0.0703 nm.

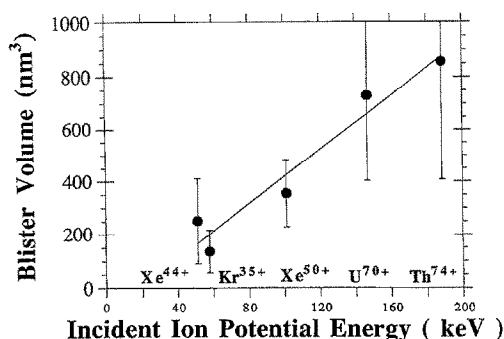


Fig. 4. Volume size of defects observed on mica as function of potential energy of incident ions at velocities of about 4×10^7 cm/s.

scan. No significant changes in the measured profiles were found when the direction of the scan was reversed. The present data suggest then that this peeling process is an exception rather than the normal behavior of these samples and its origin is still under investigation.

In the case of U^{70+} ion impact, shown in Fig. 2a, the observed height of the “blisters” is similar to that observed for Xe, though the diameter of the “blisters” is drastically increased to about 40 nm, roughly proportional to the increase in incident charge for U^{70+} compared to Xe^{44+} . No detectable “blister” defect structures were measured in the unexposed areas of any of the mica samples, as shown in Fig. 2b. Fig. 3 shows a cross section through the blisters for the Kr^{35+} case and the width and height data for that particular scan. Though the absolute dimensions of the blisters is difficult to ascertain due to the convoluting effects of the tip geometry and systematic variations due to the stiffness of the cantilever used, it has clearly been found that the relative volume of the blisters increases with increasing incident charge state for the ions studied thus far (Kr^{35+} , Xe^{44+} , Xe^{50+} , U^{70+} , Th^{74+}). The increase in volume size is shown in Fig. 4 where the “Blister” size is plotted versus the total potential energy and the electron emission per ion. The size distributions have been reproducible for each incident ion for several different AFM scans, for given probe tip and sample conditions. The quantitative relationship between the size distribution of the defects and the incident ion charge is currently under investigation.

AFM measurements did not detect any blister or pit formation for the case of Xe^+ (300 keV) [10] ion impact on mica, even for doses of some 10^{10} cm⁻². For 6 MeV/u Xe^{17+} ion impact, a large area defect is observed [10] which is inconsistent with the typical “blister” caused by the SVHCIs. Such defects have previously been observed for 7–35 MeV/u Kr ions and mica targets [11] where they have been described as characteristic “hollows” or recessed regions of reduced

mechanical strength. In such cases, the defect is due to the large kinetic energy deposited by the incident ions to the target electrons and the mechanism of defect production is similar to that induced by multiple photons using high power laser beams. Indeed, similar defects are observed in laser sputtering studies (e.g. ref. [12]). Briere et al. [13] have investigated the range of Xe^{q+} with $q = 1-44$ at impact energies of 300 keV in thermal silicon dioxide. They found that the range is essentially independent of the charge state and is about 100 nm, in agreement with semi-empirical theories such as TRIM [13], and is predominantly determined by the nuclear stopping power. These results suggest that “blister” defect formation is not related to the kinetic energy transfer, but rather to the potential energy of the incident ion, implying the following physical picture for the production of these new surface defects caused by SVHCIs, as reported here.

As the highly charged ion approaches the surface, it draws electrons out at fairly large distances ($\geq 30 a_0$) [8,9] through the lowering of the work function of the solid surface, promoting resonant electron transfer over the surface barrier into high lying Rydberg states of the incident ion. It has been found, for instance, that Xe^{44+} (4×10^7 cm/s) causes the emission of about 90 electrons per ion incident on a metallic surface, with 170 electrons being emitted per incident Th^{70+} ion of the same velocity [4,15]. The high lying Rydberg states thus formed partially neutralize the ions, still maintaining its empty core (“hollow” atom [16]). At close inter-nuclear distances (surface penetration), inner-shells (M, N shells here) are filled and a fast atomic decay process takes place, while the electrons in high n-states are stripped away [17] creating second, more compressed hollow atom in the solid, which is believed to survive for about another 1–100 fs. The emission of high energy X-rays and Auger electrons in this phase causes the dissipation of the potential energy of the ions, until the ions finally reach their ground state. However, whereas the decay of atomic inner-shell vacancies is relatively fast (ca. 10^{-14} s), the energy conversion into phonons should be much slower (ca. 10^{-13} to 10^{-12} s). The dissipation of the potential energy of the ions via electronic processes occurs in the first few monolayers and the effects on the target atoms depend on the available energy. Ions with an incident velocity of ca. 10^7 cm/s travel about 1 nm during the inner-shell vacancy decay. Strong local excitation of the target electrons or ionization of the target atoms due to the excessive electrostatic potential of the incident ion may cause Coulombic repulsion induced displacements of neighboring target atoms, producing permanent displacements. This mechanism is intimately related to that responsible for ionic tracks in insulators, formed by the passage of high energy (10’s MeV/u) ions in insulators, known as Coulomb explosions [18]. It is

interesting to note that it is not necessary to remove the target electrons to the vacuum level (ionization), rather sufficient excitation of the binding electrons can also promote atomic motion. Calculations [14] show that, for the ions of current interest, the *average* energy transfer due to Coulomb collisions between the highly charged ion and the low charge state target atoms is insufficient (< 0.1 eV) to cause such atomic displacement of the target atom. The mechanism responsible for the defect production is likely due to the surface electron emission caused by the electrostatic field of the incident highly charged ion. In mica, the electron emission would change the local charge balance between adjacent Al–Si–O layers, causing a repulsion between the layers and the intermediate positive ions (e.g. K^+) in the mica structure. This can explain the very locally confined “popping” of the first two layers, which results in the observed hollow “blisters”. The increased repulsive potential between two layers can reach several eV, depending on the number of electrons emitted and the volume from which they were emitted.

The results of these experimental findings suggest that, for insulators, single highly charged ions do, in fact, cause nanometer size surface defects via electronic processes. The “strength” of the electronic processes appears to be determined by the residual potential energy of the slow highly charged ions (fields ca. 10^8 V/cm). The incident charge and ion velocity determine the electron emission and therefore the local electrostatic defect production mechanism. Electron emission is known to increase with decreasing incident (perpendicular) velocity of the ion to the surface [8,9,15], toward the point at which the velocity at incidence is determined by the image charge [15,19,20]. If the ions are sufficiently swift (several MeV/u), kinetic energy transfer effects become dominant (electronic stopping).

Additional studies of 300 keV Xe^{44+} ion irradiation of LEXAN have also revealed “blister” formation. The defects in LEXAN have heights of about 6–7 nm and base diameters of about 40–60 nm. Again, unirradiated areas of these samples were free from such defect features. As these insulators do not possess layered structures, these cases are strong additional evidence for the production of mutual Coulombic repulsion induced collective displacement of target atoms (i.e. explosions) due to the effects of extremely large potential fields of incident slow highly charged ions.

4. Conclusion

High potential energy deposition in the first few atomic layers of an insulating surface, due to the

impact of a single slow highly charged ion, is observed via the formation of nanosize defects. These new surface defects are caused by electronic processes, primarily via emission of electrons due to the high charge of the incident ions, and via repulsive electrostatic forces associated with the subsequent charge imbalance between target atoms. The processes which cause the defects are effective within the first monolayers of the surface region. The sizes of the defects are strongly dependent upon the total potential energy of the incident ions.

Acknowledgment

This work was performed under the auspices of the U.S. Department of Energy by the Lawrence Livermore National Laboratory under contract W-7405-ENG-48.

References

- [1] M.A. Levine, R.E. Marrs, J.R. Henderson, D.A. Knapp, and M.B. Schneider, *Phys. Scripta* T 22, (1988) 17; M.A. Levine, *Nucl. Instr. and Meth. B* 43 (1989) 431.
- [2] D. Schneider, D. DeWitt, M.W. Clark, R. Schuch, C.L. Cocke, R. Schmieder, K.J. Reed, M.H. Chen, R. Marrs, M. Levine and D. Fortner, *Phys. Rev. A* 42 (1990) 389.
- [3] D.H. Schneider, M. Clark, B.M. Penetrante, J. McDonald, D. DeWitt, and J.N. Bardsley, *Phys. Rev. A* 44 (1991) 3119.
- [4] J. McDonald, D. Schneider, M. Clark and D. DeWitt, *Phys. Rev. Lett.* 46 (1992) 2297.
- [5] M. Clark, D. Schneider, D. DeWitt, M. McDonald, R. Bruch, U.I. Safronova, I.Yu. Tolstikhina and R. Schuch, *Phys. Rev. A* 47 (1993) 3989.
- [6] S.T. De Zwart, T. Fried, D.O. Boerma, R. Hoekstra, A.G. Drentje and A.L. Boers, *Surf. Sci.* 177 (1986) L939.
- [7] G. Schiwietz, D. Schneider, M.W. Clark, B. Skogvall, D. DeWitt, and J. McDonald, *Radiat. Eff. and Def. Solids* 127 (1993) 11.
- [8] N. Bardsley and B.M. Penetrante, *Comments At. Mol. Phys.* 27 (1991) 43.
- [9] J. Burgdorfer, P. Lerner and F. Meyer, *PRA* 44 (1991) 5674.
- [10] The ion-beams for these measurements were provided by the Hahn-Meitner-Institut Van de Graaff (Xe^+) and the Texas A&M cyclotron accelerators; private communication, D. Schneider.
- [11] F. Thibaudau, J. Cousty, E. Balanzat and S. Bouffard, *Phys. Rev. Lett.* 67 (1991) 1582.
- [12] R. Kelly, J.J. Cuomo, P.A. Leary, J.E. Rothenberg, B.E. Braren and C.F. Aliottce, *Nucl. Instr. and Meth. B* 9 (1985) 329.
- [13] M.A. Briere, J. Biersack, D. Schneider and N. Stohlfert, to be published.
- [14] J.P. Biersack and L. Hagmark, *Nucl. Instr. and Meth.* 174 (1980) 257.

- [15] F. Aumayr, H. Kurz, D. Schneider, M.A. Briere, J.W. McDonald, C. Cunningham and H.P. Winter, to be published.
- [16] J.P. Briand, L. deBilly, P. Charles, S. Essabaa, P. Briand, R. Geller, J.P. Declaux, S. Bliman and C. Ristori, PRL 65 (1990) 159.
- [17] W. Brandt and M. Kitagawa, Phys. Rev. B 25 (1982) 5631.
- [18] R.L. Fleischer, P.B. Price and R.M. Walker, J. Appl. Phys. 36 (1965) 3645.
- [19] H. Winter, Comments At. Mol. Phys. 26 (1991) 287.
- [20] J. Burgdorfer and F. Meyer, Phys. Rev. A 47 (1993) R210.